



HAL
open science

Intraseasonal variability of the West African monsoon

Serge Janicot, Guy Caniaux, Fabrice Chauvin, Gaëlle de Coëtlogon, Bernard Fontaine, N. M.J. Hall, George N. Kiladis, Jean-Philippe Lafore, Christophe Lavaysse, Samantha L. Lavender, et al.

► **To cite this version:**

Serge Janicot, Guy Caniaux, Fabrice Chauvin, Gaëlle de Coëtlogon, Bernard Fontaine, et al.. Intraseasonal variability of the West African monsoon. *Atmospheric Science Letters*, 2011, 12 (1), pp.58-66. 10.1002/asl.280 . hal-00548109

HAL Id: hal-00548109

<https://hal.science/hal-00548109>

Submitted on 9 Dec 2020

HAL is a multi-disciplinary open access archive for the deposit and dissemination of scientific research documents, whether they are published or not. The documents may come from teaching and research institutions in France or abroad, or from public or private research centers.

L'archive ouverte pluridisciplinaire **HAL**, est destinée au dépôt et à la diffusion de documents scientifiques de niveau recherche, publiés ou non, émanant des établissements d'enseignement et de recherche français ou étrangers, des laboratoires publics ou privés.

Intraseasonal variability of the West African monsoon

S. Janicot,^{1*} G. Caniaux,² F. Chauvin,² G. de Coëtlogon,³ B. Fontaine,⁴ N. Hall,⁵ G. Kiladis,⁶ J.-P. Lafore,² C. Lavaysse,⁷ S. L. Lavender,⁸ S. Leroux,⁶ R. Marteau,⁴ F. Mounier,⁹ N. Philippon,⁴ R. Roehrig,² B. Sultan¹ and C. M. Taylor¹⁰

¹Laboratoire d'Océanographie et du Climat: Expérimentation et Analyses Numériques/Institut Pierre-Simon Laplace, Institut de Recherches pour le Développement, Université Pierre et Marie Curie, Boite 100, 75252 Paris cedex 05, France

²Centre National de Recherches Météorologiques, Météo-France, Toulouse, France

³Laboratoire Atmosphères, Milieux, Observations Spatiales/Institut Pierre-Simon Laplace, Université Pierre et Marie Curie, Paris, France

⁴Centre de Recherches de Climatologie, Université de Bourgogne, Dijon, France

⁵Laboratoire d'Etudes en Géophysique et Océanographie Spatiales/Observatoire Midi-Pyrénées, Toulouse, France

⁶Physical Sciences Division, Earth System Research Laboratory, National Oceanic and Atmospheric Administration, Boulder, Colorado, USA

⁷Mac Gill University, Montreal, Canada

⁸School of Environmental Sciences, University of East Anglia, Norwich, UK

⁹EQECAT, Paris, France

¹⁰Centre for Ecology and Hydrology, Wallingford, UK

*Correspondence to:

S. Janicot, LOCEAN/IPSL,
Université Pierre et Marie Curie,
Boite 100, 4 Place Jussieu,
75252 Paris cedex 05, France.
E-mail:
serge.janicot@locean-ipsl.upmc.fr

Abstract

The intraseasonal time scale is critical in West Africa where resources are highly rainfall dependent. Three main modes of variability have been identified, two with a mean periodicity of 15 days and one with a mean periodicity around 40 days. These modes have a regional scale and can strongly influence precipitation and convective activity. They are mainly controlled by atmospheric dynamics and land–surface interactions. They can also modulate the very specific phase of the African summer monsoon onset. A better knowledge of the mechanisms controlling this scale is necessary to improve its predictability. Copyright © 2010 Royal Meteorological Society

Keywords: West African monsoon; intraseasonal variability; monsoon onset; predictability; crop yield

Received: 9 February 2010

Revised: 7 May 2010

Accepted: 10 May 2010

1. Background

The mean seasonal cycle of rainfall of the West African Monsoon (WAM) is presented in Figure 1 (top) through a time–latitude cross-section using the Global Precipitation Climatology Project (GPCP) data (Huffman *et al.*, 2001). The meridional displacement of the inter-tropical convergence zone (ITCZ) is not smooth but characterized by a succession of active phases and pauses. The first rainy season along the Guinean Coast is evident between mid-April and the end of June. It is followed by the summer monsoon season where the ITCZ is shifted to the north and centred over 11°N, bringing precipitation over the Sahel region. The abrupt northward shift of the monsoon at its onset time contrasts with the smooth retreat of the ITCZ. This is followed by the second rainy season over the Guinean Coast in October–November. This African monsoon onset, preceded by weakened convective activity, has been described using various data sets (Le Barbe *et al.*, 2002; Sultan and Janicot, 2003; Fontaine and Louvet, 2006; Fontaine *et al.*, 2008). It corresponds to a 10–15-day transition in the WAM seasonal evolution, and its mean date of occurrence varies depending on the variable used. Over the last 40 years its mean date is between 24 and 30 June with a standard deviation of 8 days.

The succession of active phases and pauses is a recurrent feature of the WAM. Figure 2 (bottom) shows an example of such variability using a daily *in situ* rainfall dataset from IRD (Institut de Recherches pour le Développement). Sequences of more than 10 days of persistent high or low rainfall amounts are evident. Low values occur between mid-July and mid-August. Day-to-day fluctuations are also evident, revealing the influence of the African easterly waves and the mesoscale convective systems. A wavelet diagram quantifies this variability (Figure 2 top) by identifying intermittent signals through their time occurrence and periodicity. Three period intervals are highlighted: (1) the synoptic time scale below 10 days; (2) a short intraseasonal scale between 10 and 25 days in which strong signals are detected from the beginning of June to mid-July, and around the beginning of September; (3) a long intraseasonal scale between 25 and 60 days with a strong signal in July–August.

The basic mechanisms controlling this time scale variability was mostly unknown before AMMA beginning and its predictability has not been addressed, although weather and seasonal forecasts have some skill. The main results from research over the last five years are summarized here.

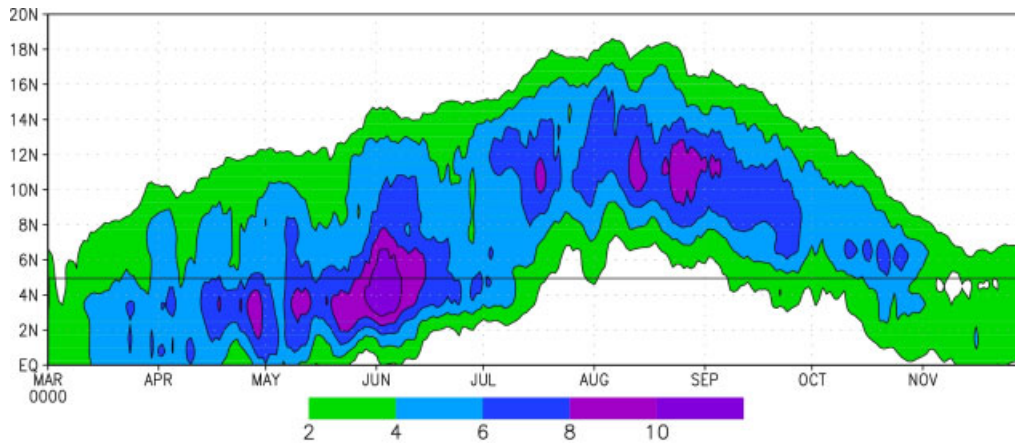


Figure 1. The mean seasonal cycle of rainfall over West Africa through a latitude cross-section. March–November daily precipitation values (mm/day) from GPCP satellite-estimated values are averaged over 5°W–5°E and over the period 1997–2006. A 7-day moving average has been applied to remove high-frequency variability. The black horizontal line at 5°N represents the Guinean Coast.

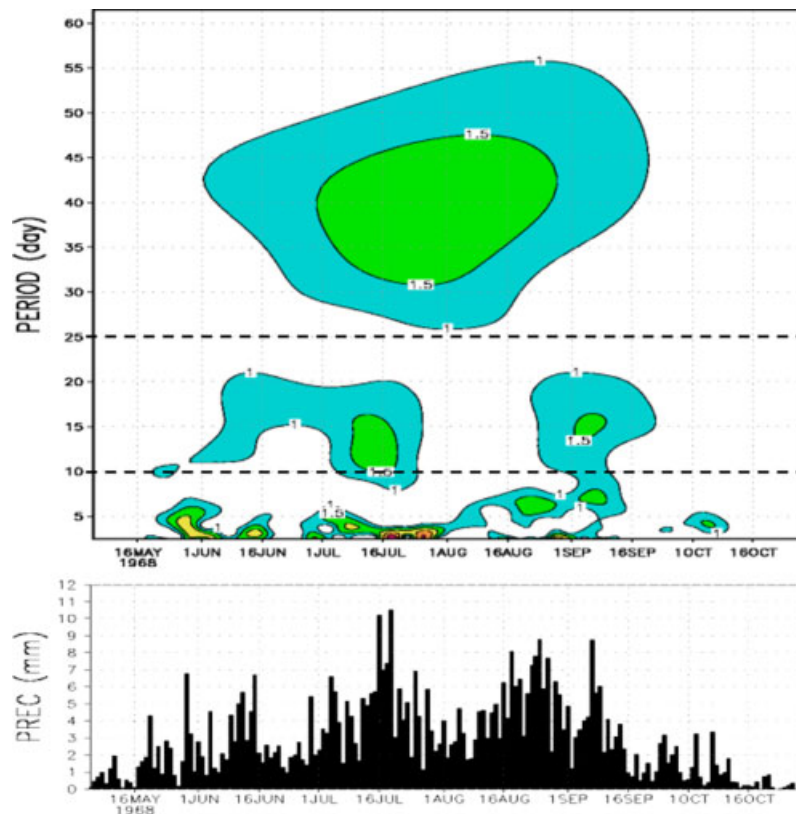


Figure 2. Bottom: Time series from 1st of May to 31st of October 1968 of daily rainfall (mm/day) averaged over the Sahel area 2.5°W–2.5°E/12.5°N–15°N. Data set from IRD *in situ* measurements. Top: Associated wavelet diagram.

2. The main modes of intraseasonal variability of convection

2.1. Detection

The daily outgoing longwave radiation (OLR) dataset produced by the Climate Diagnostic Center is a proxy for deep convection (low OLR values correspond to cold cloud tops associated with deep convective activity and high precipitation in the Tropics). Atmospheric circulation is described using the NCEP-DOE reanalysis dataset. The OLR data have been filtered to

extract 10–25- and 25–90-day signals. A decomposition of these signals has been carried out using empirical orthogonal functions, providing the main ‘modes of variability’. At the 10–25-day scale the first two modes have been retained, and the first mode at the 25–90-day scale. A composite time sequence has been computed for each mode. Strong events are selected for the days when the time series of the mode is higher than +1 standard deviation, and weak events for the days when it is lower than –1 standard deviation. The means of OLR and other variables are computed by

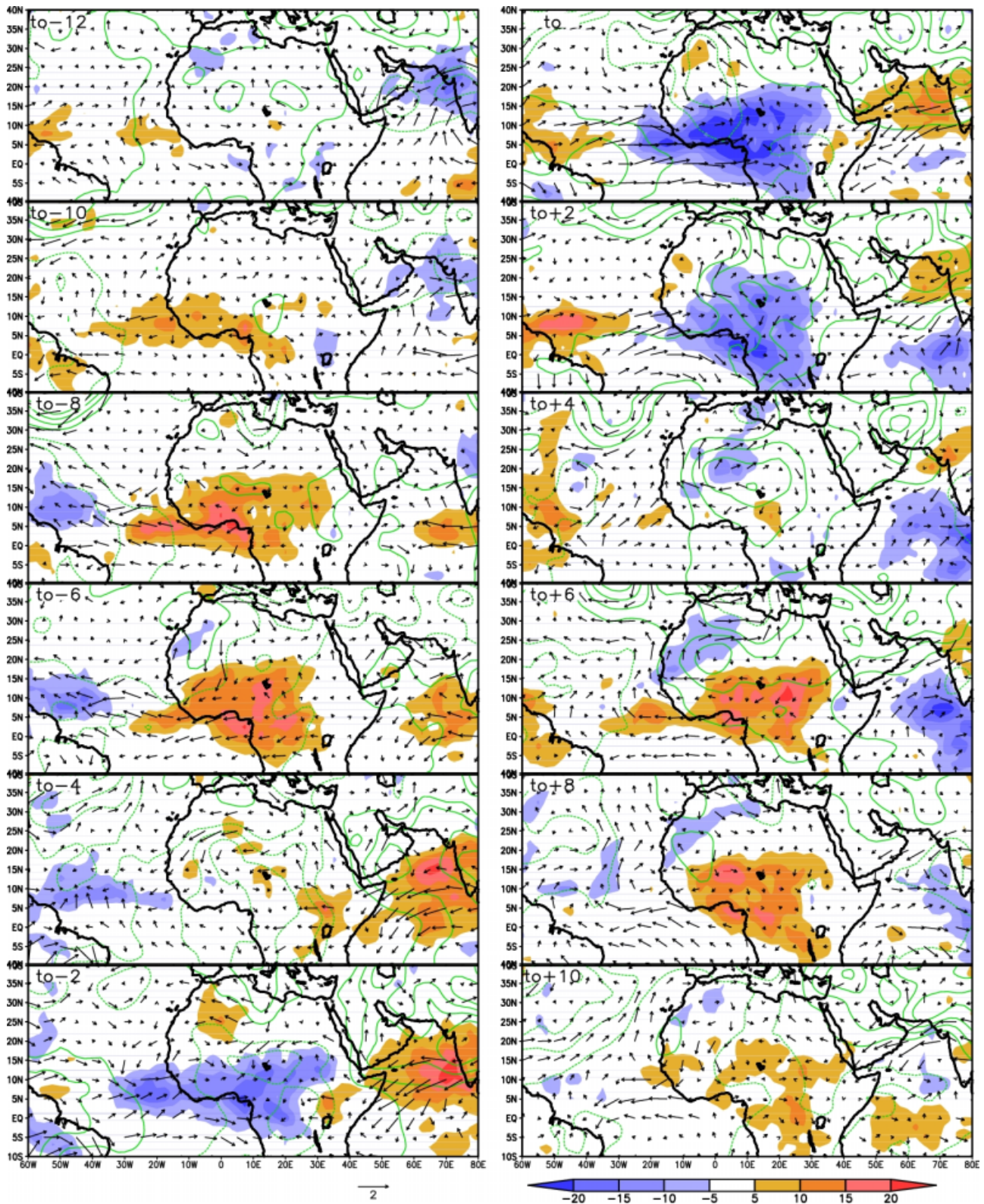


Figure 3. Time sequence of strong minus weak convective events for June–September for every year from 1979 to 2006, based on the reconstructed 10–25-day filtered OLR ITCZ index by the first EOF mode: unfiltered OLR values (colours; W/m^2), 925-hPa wind vectors (m/s) and 925-hPa geopotential heights [green solid (dashed) contours for positive (negative) values; isolines are drawn every 2 geopotential metres with zero-isoline omitted]. For clarity, only one grid point out of two is represented for the wind vectors. The sequence goes from $t_0 - 12$ to $t_0 + 10$ days with a time lag of 2 days. The convection increase is represented by blue colour, and convection decrease by red colour.

averaging all the selected days for strong and weak events, respectively. A reference time t_0 is attributed to these means. Similar means are computed for the

days before and after t_0 . The time sequences of the difference between the strong and the weak events are presented in Figures 3–5.

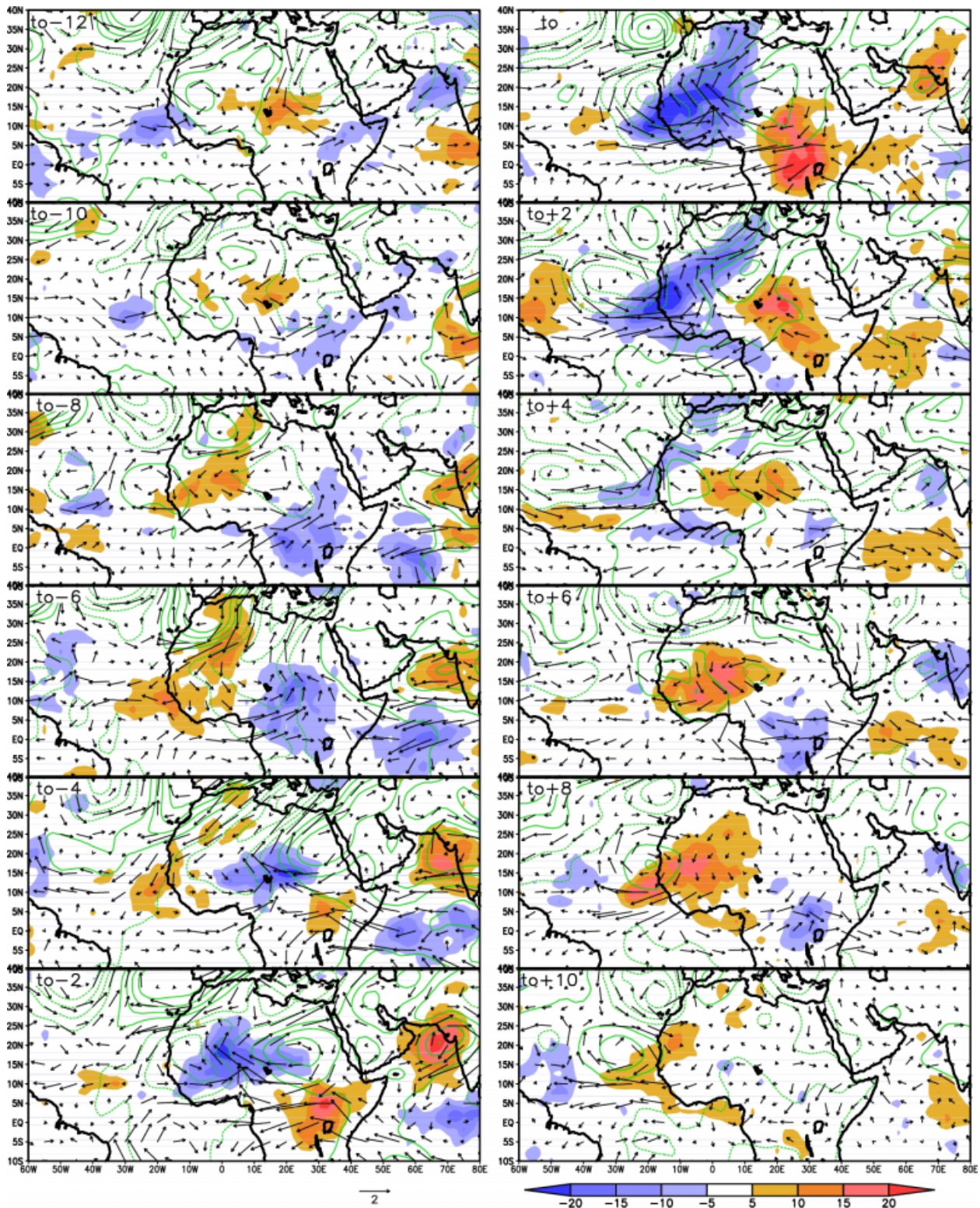


Figure 4. Time sequence of strong minus weak convective events for June–September for every year from 1979 to 2006, based on the reconstructed 10–25-day filtered OLR ITCZ index by the second EOF mode: unfiltered OLR values (colours; W/m^2), 700-hPa wind vectors (m/s) and 700-hPa geopotential heights [green solid (dashed) contours for positive (negative) values; isolines are drawn every 2 geopotential metres with zero-isoline omitted]. For clarity, only one grid point out of two is represented for the wind vectors. The sequence goes from $t_0 - 12$ to $t_0 + 10$ days with a time lag of 2 days. The convection increase is represented by blue colour, and convection decrease by red colour.

2.2. The ‘quasi-biweekly zonal dipole’ mode

The first 10–25-day mode is the ‘quasi-biweekly zonal dipole’ (QBZD; Mounier *et al.*, 2008) (Figure 3).

About 5.5 strong and weak events are detected in average per summer (June–September). This sequence shows a modulation in convection as a standing oscillation growing and decreasing over the southern

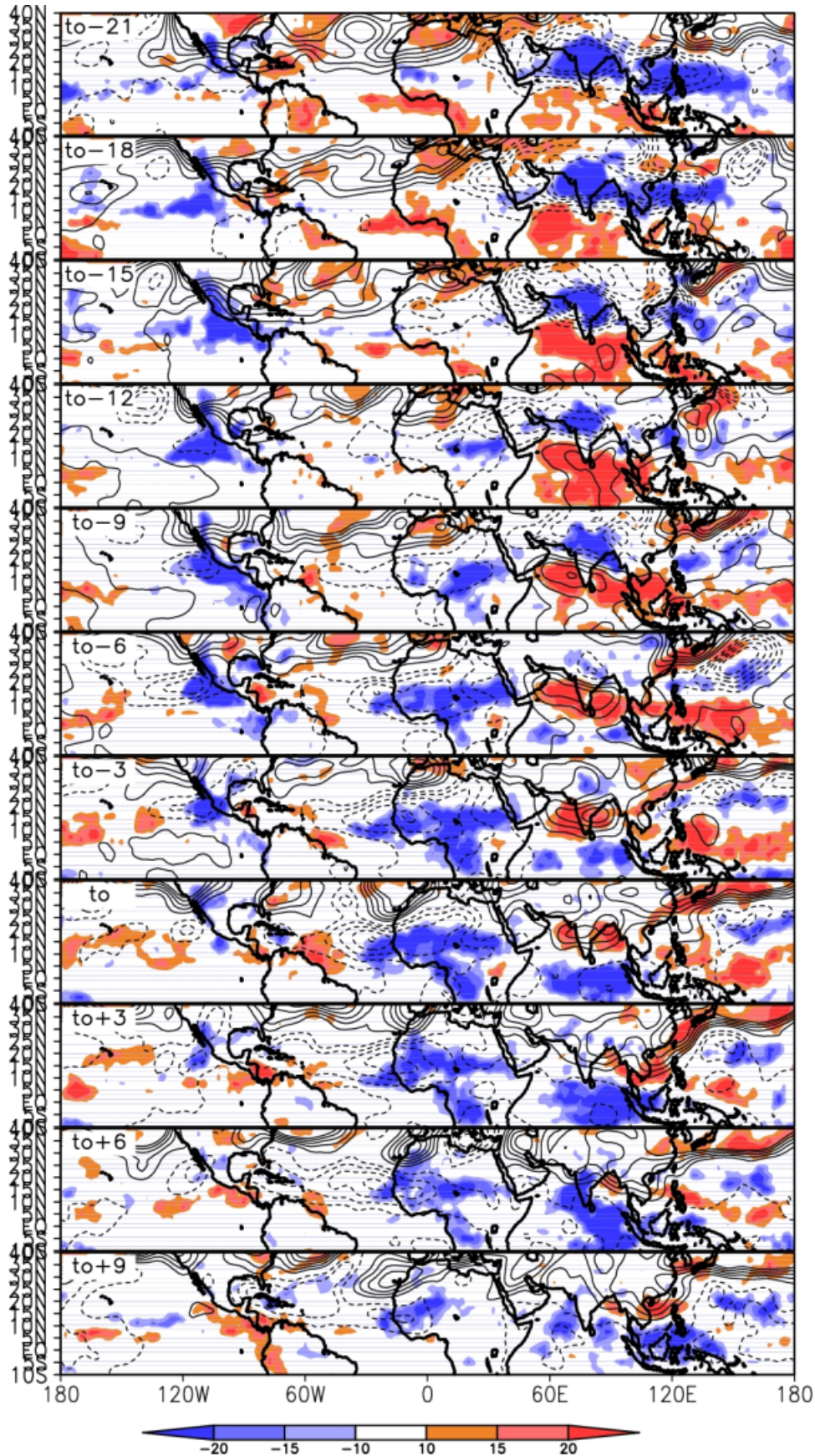


Figure 5. Time sequence of strong minus weak convective events for June–September for every year from 1979 to 2006, based on the reconstructed 25–90-day filtered OLR ITCZ index by the first EOF mode: unfiltered OLR values (colours; W/m^2) and 700-hPa geopotential heights [solid (dashed) contours for positive (negative) values; isolines are drawn every 4 geopotential metres with zero-isoline omitted]. The sequence goes from $t_0 - 21$ to $t_0 + 9$ days with a time lag of 3 days. The convection increase is represented by blue colour, and convection decrease by red colour.

coast of West Africa and over Central Africa. An opposite polarity is located over 60°W – 30°W , yielding evidence of a zonal dipole of convection. This sequence shows a mean periodicity of about 14 days since we get a similar OLR anomaly field at $(t_0 - 8)/(t_0 - 6)$ and $(t_0 + 6)/(t_0 + 8)$. The OLR anomalies propagate eastwards between these two poles of convection (see panels $t_0 - 8$ to $t_0 - 2$ in Figure 3). This signal seems to continue propagating eastwards and modulate convection over the Indian Ocean, but it is not clearly evident between Central Africa and the Indian basin. This may be due to the East African orography which separates the convective regimes over East Africa from the Indian monsoon.

The mechanisms of this dipole have been diagnosed by using NCEP-DOE reanalyses (Mounier *et al.*, 2008). Briefly, this dipole pattern appears as controlled both by equatorial atmospheric disturbances propagating eastwards and by radiation–atmosphere interaction processes over Africa. When convection is at a minimum over Africa, a lack of cloud cover results in higher net shortwave flux at the surface, increasing the surface temperature and lowering the surface pressure. This creates an east–west pressure gradient leading to an increase in eastward moisture advection inland (see the negative 925-hPa geopotential values and the reversal of the wind at $t_0 - 4$). The arrival of a positive pressure signal from the Atlantic (see at $t_0 - 2$ and t_0) amplifies the low-level westerly winds and the moisture advection inland, leading to an increase in convective activity over Africa. Then the opposite phase of the dipole develops.

2.3. The ‘Sahel’ mode

The second 10–25-day mode is the ‘Sahel’ mode (Sultan *et al.*, 2003; Janicot *et al.*, 2010) (Figure 4). About 4.5 strong and weak events are detected on average per summer. This signal initiates over the eastern equatorial Africa (see $t_0 - 12$ and $t_0 - 10$ in Figure 4), enhances in the same place ($t_0 - 8$), then moves northwards up to 15°N ($t_0 - 6$), and finally propagates westwards until it dissipates over the tropical Atlantic ($t_0 + 4$). At t_0 its greatest meridional extension is over West Africa, reaching the Mediterranean coast. This OLR extension is due to higher moisture content (so weaker longwave radiation), but not with precipitation, as it is far from the ITCZ. The mean periodicity of this mode is approximately 15 days.

The atmospheric circulation is characterized by cyclonic circulation at 700 hPa located ahead of negative OLR anomalies bringing more moisture within the enhanced convective area, and vice-versa. At $t_0 - 8$ and $t_0 - 6$, the low-level cyclonic cell moving westwards along Sahelian latitudes induces stronger southerly winds and increased moisture content east of 15°E and north of the negative OLR anomaly pole. This provides moisture conditions favourable for increased convection there and for the northward displacement of the convective envelope. From $t_0 - 4$ to

$t_0 + 2$ the westward evolution of the Sahel mode structure induces the development of an anticyclonic cell east of 10°E , which brings drier air over the equatorial Africa by northerly winds, a favourable condition for decreased convection there and for the northward development of the positive OLR anomalies.

Land–atmosphere and radiation–atmosphere interaction processes can contribute to the maintenance and the westward propagation of the Sahel mode (Taylor, 2008; Taylor, 2011). Extensive areas of wet soil associated with the positive phase of the Sahel mode induce weak surface heat fluxes and low-level anticyclonic circulation bringing moisture ahead of the convective zone and helping its westward propagation. GCM simulations with and without soil moisture coupling at intraseasonal scale suggest that this westward-propagating mode is also controlled by a purely internal atmospheric mode (Lavender *et al.*, 2009). This atmospheric mode might be due to a convectively coupled equatorial Rossby wave signal which also propagates westwards (Janicot *et al.*, 2010).

2.4. The ‘African MJO’ mode

The first 25–90-day mode is the ‘African MJO’ mode (Matthews, 2004; Janicot *et al.*, 2009) in reference to the Madden-Julian Oscillation detected over the Indian and West Pacific sectors (Figure 5). About 1.5 strong and weak events are detected on average per summer. The pattern at t_0 shows enhanced convection over most of West and Central Africa. Negative OLR anomalies begin to occur northeast of Lake Chad. They grow and propagate westwards, and dissipate over the western part of Africa. At the same time an MJO-type signal is evident over the Indian – West Pacific sector, characterized by a meridional dipole of convection moving northwards. At $t_0 - 18$ a positive OLR anomaly is located at the equator while convection is enhanced over India, corresponding to an active phase of the Indian monsoon. The equatorial positive OLR anomaly grows and reaches India around $t_0 - 10$ consistent with the occurrence of a break in the Indian monsoon up to t_0 . Then an active phase begins with the northward propagation of the following negative OLR anomaly.

Matthews (2004) suggested that equatorial dry Kelvin waves and dry Rossby waves could link the MJO in the Indian sector and the African MJO mode. Twenty days prior to an enhancement of convection over Africa, MJO convection is decreasing over the equatorial warm pool. In response a dry equatorial Kelvin wave propagates eastwards and a dry equatorial Rossby wave response propagates westwards. They complete a circuit of the equator and meet 20 days later over Africa favouring an enhancement of deep convection. However, the African MJO mode is characterized by a westward propagation, suggesting that a convectively coupled equatorial Rossby wave signal

is dominant (Janicot *et al.*, 2009, 2010; Lavender and Matthews, 2009).

This westward moving signal is also preceded by the development of low geopotential associated with enhanced convection over northern India around $t_0 - 20$. This cyclonic circulation extends westwards in the following days reaching West Africa at $t_0 - 15$. It contributes to the disappearance of the positive OLR anomaly pattern by enhancing westerly moisture advection inland, and to the development of the enhanced convection envelope over Africa associated with the African MJO mode. Then the break phase occurs over India, accompanied by a high geopotential which later moves westwards and contributes to the disappearance of the African MJO mode. So both convectively coupled equatorial Rossby waves and Indian monsoon active and break phases contribute to the African MJO mode.

3. The predictability of intraseasonal variability and monsoon onset

The first potential factor for the monsoon onset is the establishment and the development of the cold tongue in the gulf of Guinea starting in mid-April and resulting from atmospheric forcing in this area and oceanic processes (Brandt *et al.*, 2011; Coëtlogon *et al.*, 2010). This enhances the meridional temperature gradient between the ocean and the continent and favours the ITCZ rainfall over the Guinean Coast. Aside the continuous cooling in the Guinea gulf, the following factor for the monsoon onset is the solar radiative forcing which increases gradually over the northern tropics, enhancing thermal and moisture contrasts with the Guinea gulf and the tropical Atlantic on the west. This contributes to the establishment of the Saharan heat low between the Atlas and Hoggar highs in mid-June, also linked to the surface albedo distribution in this area (Sultan and Janicot, 2003; Ramel *et al.*, 2006; Lavaysse *et al.*, 2009). This leads to the enhancement of the low-level westerly moisture advection off the West African coast, feeding convection in the ITCZ along 10°N . The enhancement of this low-level westerly jet may also create an inertially unstable environment, favouring the abrupt northward shift of the monsoon (Hagos and Cook, 2007). This shift is evident where the low-level gradients are strong, that is mainly between 10°W and 10°E . However, it has also been shown that large-scale intraseasonal events like the African MJO mode could have a role in the African monsoon onset as in 2006 during the AMMA intensive field campaign (Janicot *et al.*, 2008).

From this knowledge some progress has been made in terms of monsoon onset date predictability, even if a more precise evaluation is still needed. Fontaine and Louvet (2006) and Fontaine *et al.* (2008) showed that it is possible to explain a high level of variance of the onset dates some weeks in advance by

performing multivariate linear regressions based on regional atmospheric predictors. Brandt *et al.* (2011) also found significant correlations 20 days in advance between the date when the cold tongue area reaches $400\,000\text{ km}^2$ and the monsoon onset date. More generally, Sultan *et al.* (2009) studied the predictability of the 10–90-day intraseasonal variability of precipitation and of the main individual modes using either a statistical approach or the dynamical forecasts scheme of ECMWF. They showed that in a hindcast context the statistical predictability at 5 and 10 days can be high, especially when the characteristics of the associated intraseasonal modes of precipitation are well defined. In an operational context, both statistical and dynamical precipitation forecast skills of the 10–90 intraseasonal band are low but predictability of individual intraseasonal modes is higher. Using dynamical variables usually more reliable than rainfall could help improving this skill.

4. Links with applications

The African monsoon brings most of the total annual rainfall in only few months. So sub-Saharan African crop yields, water resources and livestock farming, which are strongly rainfall dependent, can be greatly affected by the timing and the intensity of monsoon irregularities. Derived from agronomic simulations, the regional onset of the monsoon is very close to the ideal sowing date in the Sahel because it minimizes the risk of a dry spell just after the sowing. When the simulated yields using the monsoon onset criterion are low, this is generally caused by intraseasonal dry spells that have different impacts depending on phenological stage of the crop (Sultan *et al.*, 2005). A dry spell on the 25–90-day scale can have a dramatic impact on the crop yield. On the other hand, the seasonal total of precipitation shows a weaker impact on average, especially at the local scale. The intraseasonal variability within a monsoon season does not appear to be correlated to the seasonal rainfall amount.

The spatial scale issue is critical. Interannual variability of the local-scale monsoon onset is not strongly spatially coherent (Marteau *et al.*, 2008). The amount of common signal across the rainfall stations in the Sahel is weaker than the interstation noise. A systematic spatially consistent advance or delay of the onset is hardly ever observed across the Sahel. Translating global climate model outputs into attainable crop yields is difficult because the model grid boxes are of larger scale than the processes governing yield, which involve the partitioning of rain between runoff, evaporation, transpiration, drainage and storage at the plot scale (Baron *et al.*, 2005). Efficient downscaling process (Paeth *et al.*, 2011) must be applied to generate local rain patterns from grid cell means and restore the variability lost by aggregation.

5. Conclusion and perspectives

In the framework of the AMMA project, and using available multi-year datasets, a broader understanding of intraseasonal variability in the African monsoon has been achieved, although a comprehensive view is still lacking. The main modes of variability at these time scales have been identified. They have a regional extension and represent an envelope modulating the convective activity of individual systems. These modes are intermittent but their impact on precipitation and convective activity is strong when they occur. They have a marked zonal propagation character, westward for the MJO and Sahel modes, and eastward for the QBZD mode, although its stationary component is important over Africa. These modes are controlled both by internal atmospheric dynamics and land–surface interactions. They can also have an impact on the African summer monsoon onset characterized by an abrupt northward shift of the ITCZ.

More investigation is needed on these issues. For instance, internal atmospheric processes like transient-mean flow interactions between the African easterly jet and the African easterly waves can produce convection fluctuations at intraseasonal time scales (Cornforth *et al.*, 2009; Leroux *et al.*, 2009). These modes are also a source and a part of some teleconnection mechanisms, with the Indian monsoon sector and with the extra-tropics and the Mediterranean sector as shown by Vizzy and Cook (2009) and Chauvin *et al.* (2010). These intraseasonal modes probably also have strong impacts during the other seasons of the year when the ITCZ is close to or over the equator, favouring interactions between equatorial atmospheric dynamics and convection. A better knowledge of the mechanisms controlling this scale is necessary to improve its predictive skill and be able to respond to the main requirements of farmers and stake-holders (Genesio *et al.*, 2011; Traore *et al.*, 2011).

Acknowledgements

The support of the AMMA project is gratefully acknowledged (see <http://onlinelibrary.wiley.com/doi/10.1002/asl.331/full> for full acknowledgement).

References

- Baron C, Sultan B, Balme M, Sarr B, Traore S, Lebel T, Dingkuhn M, Janicot S. 2005. From GCM grid cell to agricultural plot: Scale issues affecting modelling of climate impact. *Philosophical Transactions of the Royal Society* **360**: 2095–2108, DOI:10.1098/rstb.2005.1741.
- Brandt P, Caniaux G, Bourles B, Lazar A, Dengler M, Funk A, Hormann V, Giordani H, Marin F. 2011. Equatorial upper-ocean dynamics and their interaction with the West African monsoon. *Atmospheric Science Letters* **12**: 24–30, DOI: 10.1002/asl.287.
- Chauvin F, Roehrig R, Lafore J-P. 2010. Intraseasonal variability of the Saharan heat low and its link with mid-latitudes. *Journal of Climate* in press.
- Coëtlogon GS, Janicot S, Lazar A. 2010. Intraseasonal variability of the ocean-atmosphere coupling in the gulf of Guinea during northern spring and summer. *Quarterly Journal of the Royal Meteorological Society* **136**: 426–441, DOI:10.1002/qj.554.
- Cornforth R, Thorncroft C, Hoskins B. 2009. The impact of moist processes on the African easterly jet – African easterly wave system. *Quarterly Journal of the Royal Meteorological Society* **135**: 894–913.
- Fontaine B, Louvet S. 2006. Sudan-Sahel rainfall onset: definition of an objective index, types of years, and experimental hindcasts. *Journal of Geophysical Research* **111**: DOI: 10.1029/2005JD007019.
- Fontaine B, Louvet S, Roucou P. 2008. Definition and predictability of an OLR-based West African monsoon onset. *International Journal of Climatology* **13**: 1787–1798, DOI: 10.1002/joc.1674.
- Genesio L, Bacci M, Baron C, Diarra B, Di Vecchia A, Alhassane A, Hassane I, Ndiaye M, Philippon N, Tarchiani V, Traoré S. 2011. Early warning systems for food security in West Africa: evolution, achievements and challenges. *Atmospheric Science Letters* **12**: 142–148, DOI: 10.1002/asl.332.
- Hagos SM, Cook KH. 2007. Dynamics of the West African monsoon jump. *Journal of Climate* **20**: 5264–5284.
- Huffman GJ, Adler RF, Morrissey MM, Bolvin DT, Curtis S, Joyce R, McGavock B, Susskind J. 2001. Global precipitation at one-degree daily resolution from multisatellite observations. *Journal of Hydrometeorology* **2**: 36–50.
- Janicot S, Thorncroft CD, Ali A, Asencio N, Berry G, Bock O, Bourles B, Caniaux G, Chauvin F, Deme A, Kergoat L, Lafore JP, Lavaysse C, Lebel T, Marticorena B, Mounier F, Nedelec P, Redelsperger JL, Ravegnani F, Reeves CE, Roca R, de Rosnay P, Schlager H, Sultan B, Tomasini M, Ulanovsky A. 2008. Large scale overview of the summer monsoon over the summer monsoon in West Africa during the AMMA field experiment in 2006. *Annales Geophysicae* **26**: 2569–2595.
- Janicot S, Mounier F, Hall N, Leroux S, Sultan B, Kiladis G. 2009. The West African monsoon dynamics. Part IV: Analysis of 25–90-day variability of convection and the role of the Indian monsoon. *Journal of Climate* **22**: 1541–1565.
- Janicot S, Mounier F, Gervois S, Sultan B, Kiladis G. 2010. The dynamics of the West African monsoon. Part V: The role of convectively coupled equatorial Rossby waves. *Journal of Climate* DOI: 10.1175/2010JCLI3221.1.
- Lavaysse C, Flamant C, Janicot S, Parker D, Lafore J-P, Sultan B, Pelon J. 2009. Seasonal cycle of the West African heat low: a climatological perspective. *Climate Dynamics* **33**: 313–330, DOI:10.1007/s00382-009-0553-4.
- Lavender SL, Matthews AJ. 2009. Response of the West African monsoon to the Madden-Julian oscillation. *Journal of Climate* **22**: 4097–4116, DOI:10.1175/2009JCLI2773.1.
- Lavender SL, Taylor CM, Matthews AJ. 2009. Coupled land-atmosphere intraseasonal variability of the West African monsoon in a GCM. *Journal of Climate* (submitted).
- Le Barbe L, Lebel T, Tapsoba D. 2002. Rainfall variability in West Africa during the years 1950–90. *Journal of Climate* **15**: 187–202.
- Leroux S, Hall NMJ, Kiladis GN. 2009. A climatological study of transient-mean flow interactions over West Africa. *Quarterly Journal of the Royal Meteorological Society* **136**: 397–410.
- Marteau R, Moron V, Philippon N. 2008. Spatial coherence of monsoon onset over Western and Central Sahel (1950–2000). *Journal of Climate* **22**: 1331–1342.
- Matthews AJ. 2004. Intraseasonal variability over tropical Africa during northern summer. *Journal of Climate* **17**: 2427–2440.
- Mounier F, Janicot S, Kiladis GN. 2008. The West African monsoon dynamics. Part III: The quasi-biweekly zonal dipole. *Journal of Climate* **21**: 1911–1928.
- Paeth H, Hall NMJ, Gaertner MA, Alonso MD, Moumouni S, Polcher J, Ruti PM, Fink AH, Gosset M, Lebel T, Gaye AT, Rowell DP, Moufouma-Okia W, Jacob D, Rockel B, Giorgi P, Rummukainen M. 2011. Progress in regional downscaling of West African precipitation. *Atmospheric Science Letters* **12**: 75–82, DOI: 10.1002/asl.306.
- Ramel R, Galle H, Messenger C. 2006. On the northward shift of the west African monsoon. *Climate Dynamics* **26**: 429–440.

- Sultan B, Janicot S. 2003. The West African monsoon dynamics. Part II: the “preonset” and “onset” of the summer monsoon. *Journal of Climate* **16**: 3389–3406.
- Sultan B, Janicot S, Diedhiou A. 2003. The West African monsoon dynamics. Part I: Documentation of intraseasonal variability. *Journal of Climate* **16**: 3407–3427.
- Sultan B, Baron C, Dingkuhn M, Janicot S. 2005. Agricultural impacts of large-scale variability of the West African monsoon. *Agricultural and Forest Meteorology* **128**: 93–110.
- Sultan B, Correia S, Janicot S. 2009. Medium-lead prediction of intraseasonal oscillations in West Africa. *Weather and Forecasting* **24**: 767–784, DOI:10.1175/2008WAF2222155.1.
- Taylor CM. 2008. Intraseasonal land-atmosphere coupling in the West African monsoon. *Journal of Climate* **21**: 6636–6648.
- Taylor CM, Parker DJ, Kalthoff N, Gaertner MA, Philippon N, Bastin S, Harris PP, Boone A, Guichard F, Agusti-Panareda A, Baldi M, Cerlini P, Descroix L, Douville H, Flamant C, Grandpeix J-Y, Polcher J. 2011. New perspectives on land-atmosphere feedbacks from the African Monsoon Multidisciplinary Analysis. *Atmospheric Science Letters* **12**: 38–44, DOI: 10.1002/asl.336.
- Traore SB, Alhassane A, Muller B, Kouressy M, Some L, Sultan B, Oettli P, Siéné Laopé AC, Sangaré S, Vaksman M, Diop M, Bégué A, Dingkhun M, Baron C. 2011. Characterizing and modelling the diversity of cropping situations under climatic constraints in West Africa. *Atmospheric Science Letters* **12**: 89–95, DOI: 10.1002/asl.295.
- Vizy EK, Cook KH. 2009. A mechanism for African monsoon breaks: Mediterranean cold air surges. *Journal of Geophysical Research* **114**: D01104, DOI:10.1029/2008JD010654.